THE JOURNAL OF PHYSICAL CHEMISTRY Letters

Letter

pubs.acs.org/JPCL

Infrared Spectral Signatures of Surface-Fluorinated Graphene: A Molecular Dynamics Study

Akira Ueta,*[,†] Yoshitaka Tanimura,*[,†] and Oleg V. Prezhdo*[,‡]

[†]Department of Chemistry, Graduate School of Science, Kyoto University, Kitashirakawa, Sakyoku, Kyoto 606-8502, Japan

[‡]Department of Chemistry, University of Rochester, RC Box 270216, Rochester, New York 14627-0216, United States

ABSTRACT: Fluorination of graphene and other carbon nanostructures is used extensively as a tool for tuning graphene's mechanical, electronic, and optical properties, and as an intermediate step in graphene functionalization. However, by penetrating through graphene surfaces, fluorine atoms create defects that deteriorate the desired properties. Using molecular dynamics simulation, we predict distinct infrared (IR) signatures that can be used to detect fluorination patterns and defects. We show that two strong peaks around 1000 and 1500 cm^{-1} in the IR signal in the graphene plane identify fluorine chains. Defects involving a single fluorine atom exhibit a clear IR peak at 800 cm^{-1} originating from the wagging motion of the F−C(sp3) bond. A pair of neighboring fluorines produces a unique peak at 1150 cm^{-1} arising as a result of the stretching vibration of the C(sp3)−C(sp3) bond hosting the fluorines. The reported results provide straightforward and efficient means for spectroscopic characterization of fluorinated graphene and related materials.

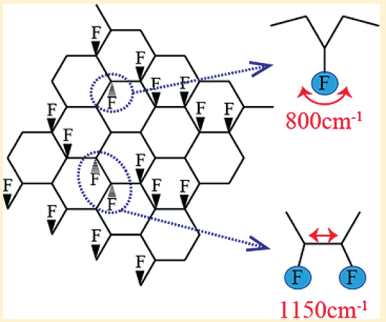

SECTION: Nanoparticles and Nanostructures

Recent discoveries and subsequent studies of fullerenes, carbon nanotubes (CNT), graphenes, and related carbon nanostructures have revealed numerous novel and often-unexpected properties that provide grounds for rapid technological advances.[1−13] For instance, quasi-one-dimensional CNTs act as miniatures antennas and exhibit enhanced field emissions, especially when the nanotube tips are opened to produces chains of linear carbons up to 100 atoms in length.[5] Two-dimensional graphene shows unusually high charge concentration and mobility, which can be induced by application of weak electric fields.[6] CNT optical properties can be tuned by diameter and helical symmetry, and the optical activity of vibrational and electronic excitations can be controlled by light polarization.[8] The exceptionally high surface area of nanoscale carbon has led to breakthroughs in the development of powerful electric batteries and capacitors.[9] Biological applications of the novel forms of carbon range from DNA sequencing[10,11] to drug delivery.[12] The former is based on the single-atom thickness and excellent conductivity of CNTs and graphene, while the latter relies on the unique combination of CNTs hydrophobic and optical properties.

Chemical modifications of nanoscale carbon broaden the spectrum of available materials and applications, and allow control over material's properties. Fluorination in particular, has produced many interesting results.[13−31] Because fluorination modifies chemical reactivity and various physical properties, multiple investigations into fluorinated carbon nanostructures have been carried out.[25−31] In contrast to graphene, which is a semimetal, fluorinated graphene (F-graphene) is a wide band gap semiconductor that is 6 orders of magnitude more resistive than graphene[28] and that luminesces in the ultraviolet.[31] It exhibits high mechanical strength, charged surfaces and local magnetic moments.[24] Mechanical, electronic, and thermodynamic properties of F-graphenes differ substantially from those of pristine graphene and scale with fluorine coverage.[21,24] Comparison of theoretical calculations with the experimental data indicates that experimental samples either contain a large number of defects or are fluorinated only partially.[29] Fluorine atoms tend to diffuse in partially F-graphenes, forming dense fluorinated lines.[22] Fluorination provides a promising chemical route for cutting graphene into smaller fragments under controlled experimental conditions.[23]

Knowledge of the arrangement of fluorine atoms poses an important problem for fluorinated CNTs, graphenes, and related nanostructures. Ordinarily, F_2 molecules are added on the outer surface of CNTs and the top surface of graphene sheets, so that all fluorine atoms are thought to be on the tube-outer and sheet-top surface. Thus, studies are often carried out under the assumption that all fluorine atoms are located on the same surface.[14,16] However, experimental evidence suggests a possibility of bonded fluorine atoms transited into the opposite side of the sheet.[19] Such transitions create strong defects, altering electrical, optical, mechanical and thermo-dynamical properties of fluorinated carbon nanostructures. These properties generally depend on the details of arrangement of fluorine atoms. In particular, multiple reports show that size, shape, curvature, and phonon modes of CNTs and graphene sheets are affected by fluorine arrangements.[5,10,13,22,23] Therefore, it is important to have a tool that can distinguish between different

Received: November 14, 2011
Accepted: January 4, 2012

   dx.doi.org/10.1021/jz201496q | J. Phys. Chem. Lett. 2012, 3, 246−250

fluorine addition structures. This goal is not easy to achieve with the current experimental methods.[18−20,25] For instance, scanning tunneling microscopy (STM) cannot access the inner fluorine atoms, while NMR and IR spectroscopies produce broad features averaged over multiple experimental structures.

In this paper, we show that various inner- and outer-surface fluorine addition structures of graphene can be differentiated using infrared (IR) spectroscopy. For this purpose, we carry out classical molecular dynamics (MD) simulations and directly calculate the IR spectroscopic response functions.

The fluorinated graphene was represented in MD using the Brenner potentials for the intramolecular C−C, C−F, and F−F interactions.[32,33] To simplify the calculation, interactions between atoms separated by more than four bond lengths were disregarded. The velocity Verlet algorithm was adopted to integrate the equation of motion with a 0.1 fs time step. The simulations were performed at around 273 K. The systems were equilibrated by repeated velocity rescaling, and energy conservation in the microcanonical trajectories following the equilibration step was confirmed. The MD trajectories were several hundred picoseconds in length. Additional information on the calculation of the IR spectra from the MD simulations, the interaction potentials including calculation of the charges on the C and F atoms, and the electric polarizability effects can be found in our previous study.[34]

Note that, due to the phenomenological interaction potential, classical MD does not necessarily give a very precise description of the structure and dynamics of fluorinated carbon nanostructures. However, the approach is sufficiently accurate to establish the differences in the IR signals for different fluorination patterns (Figure 1).

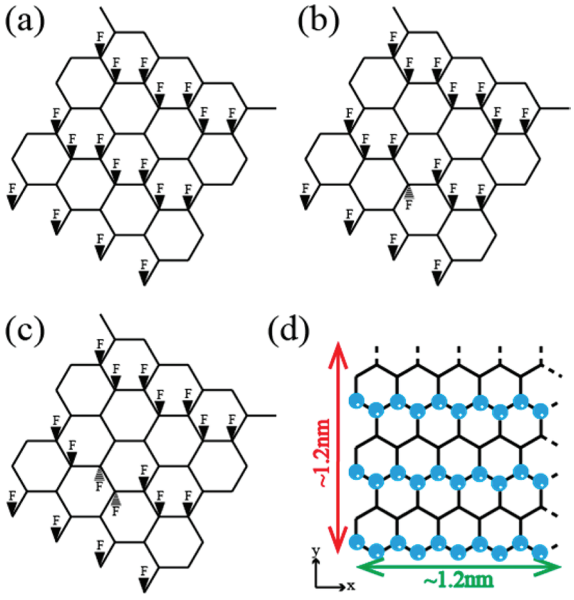

Figure 1. Three fluorinated-graphene structures: (a) with all fluorine atoms on the outer-surface of graphene, (b) with one fluorine on the inner-surface, and (c) with two fluorines on the inner-surface. (d) Simulation cell that is replicated in the x and y directions. The blue balls represent fluorine atoms. The z direction is vertical to the graphene sheet.

The study was performed using three F-graphene systems as illustrated in Figure 1a−c. Periodic boundary conditions were used. The simulation cell was 1.2 nm long, containing five benzene rings in the horizontal direction and three benzene rings in the vertical direction (Figure 1d). The system consisted of 60 carbon atoms and 30 fluorine atoms. The fluorine atoms were arranged to form an all outer-surface addition structure (Figure 1a), and two structures with one or two fluorines on the inner surface of graphene (Figure 1b,c), respectively. These structures, involving a 2:1 ratio of the numbers of carbon and fluorine atoms, with the fluorine arranged in the 1,2-position in each benzene ring, have been proposed as stable structures in many other studies.[13−16,22−26,29] We ran MD simulations to equilibrate the systems under the given conditions and checked the accuracy of the simulated structures.

Three independent polarizations of light were considered in detail, corresponding to the x, y, and z directions of the simulation cell (Figure 1d). Each IR response function was computed by averaging over an ensemble of 10^6 different initial configurations.

Figure 2 shows the computed IR spectra for light polarized along the chains of fluorine atoms, in the x direction of the

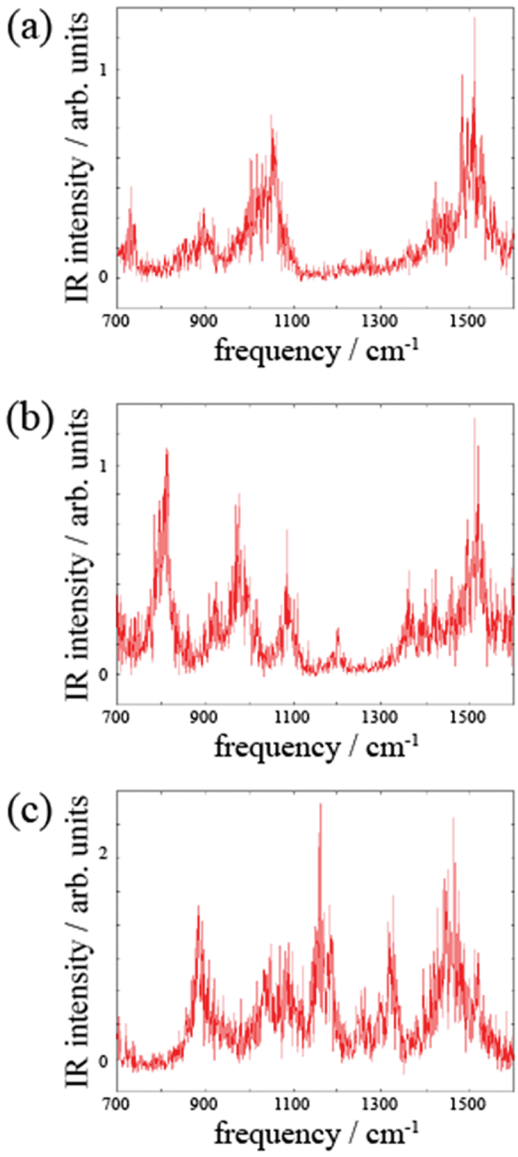

Figure 2. IR spectra obtained from full MD simulations for radiation polarized in the x direction (Figure 1d). Panels a, b, and c correspond to the all-outer, one-inner, and two-inner fluorine systems shown in panels a, b, and c of Figure 1.

dx.doi.org/10.1021/jz201496q | J. Phys. Chem. Lett. 2012, 3, 246−250

simulation cell (Figure 1d). This polarization of light leads to the largest differences in the IR signals for the all-outer, one-inner, and two-inner fluorination patterns. The peak at 800 cm^{-1} seen in Figure 2b is optically active only for the one-inner fluorine structure, whereas the peaks at 1150 and 1300 cm^{-1} appear only in the two-inner fluorine structure (Figure 2c). The *y* polarized spectra shown in Figure 3b exhibit a prominent peak at

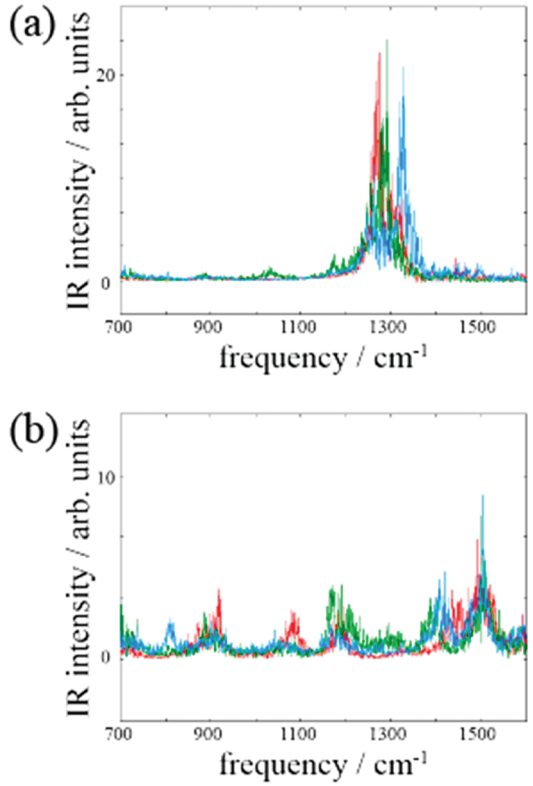

Figure 3. IR spectra obtained from full MD simulations for light polarized along (a) the *y*-direction and (b) the *z*-direction (Figure 1d). In each direction, the red line shows the all-outer, the green line shows the one-inner, and the blue line shows the two-inner fluorine systems illustrated in panels a, b, and c of Figure 1.

1300 cm^{-1}, but this peak is common in all three structures and cannot be used to distinguish between them. The *z* polarized spectra shown in Figure 3b contain a number of peaks. However, the differences between in the spectra for the three structures are rather minor, and it is difficult to distinguish the one-inner and two-inner structures from the all-outer structure. The above results indicate that one can identify a single fluorine atom on the graphene surface by focusing on the 800 cm^{-1} peak. The fluorine dimer on the graphene surface can be distinguished based on the 1150 cm^{-1} peak. The IR measurements should be taken with light polarized along the graphite surface.

In order to explore an origin for each peak in spectra, we performed a normal-mode analysis of the fluorinated graphene systems for different physical conditions. We found that the 800 cm^{-1} peak is attributed to the wagging motions of the local F−C(sp3) bond. Since the F-additions are lined up in the *x* direction, the vibrational motion of each local F−C(sp3) bond along the *x* direction are blocked. By contrast, the isolated fluorine atom on the inner surface of graphene can move along the *x* direction (Figure 4a). As a result, the 800 cm^{-1} peak is observed only in the one-inner case.

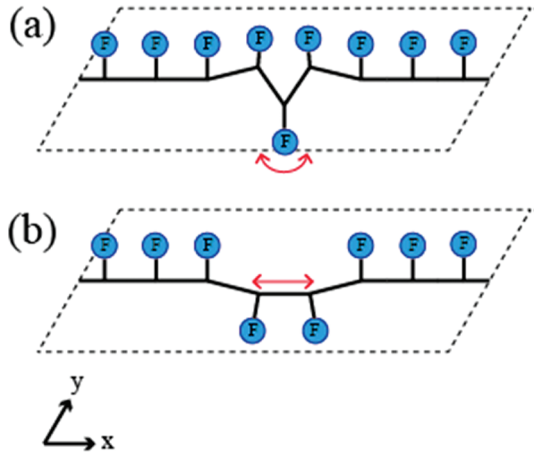

Figure 4. The schematic view of the distinct structures and characteristic vibrational modes of the one-inner and two-inner fluorine additions. Panel a illustrates the wagging motion of the local F−C(sp3) bond in the one-inner case. Panel b depicts the local C(sp3)−C(sp3) bond vibration in the two-inner case.

The peak at 1150 cm^{-1} characteristic of the fluorine dimer on the inner surface of graphene (Figure 1c), arises from the local C(sp3)−C(sp3) bond vibration along the direction of the bond (Figure 4b). Normally, C(sp3)−C(sp3) bond vibrations do not produce IR signals in nanoscale carbon materials, because these bonds are apolar. In the current case, the C(sp3)−C(sp3) vibrational motion can be detected in the IR signal through its interaction with the polar F−C(sp3) bonds. The 1150 cm^{-1} peak is distinct from the vibrations of the C(sp3) atoms bound to fluorines in the all-outer structure (Figure 1a), because the two carbons connected to the inner fluorine deviate from the plane of graphene, and therefore, differ from the other C(sp3) atoms, as indicated schematically in Figure 4b. An analogous peak is not observed in the isolated fluorine case (Figure 1b), because the two C(sp3;inner)−C(sp3;outer) bonds vibrate asymmetrically around the isolated fluorine atom (Figure 4a), and the sum of the contribution of these two bonds to the *x*-polarized IR signal cancels out.

The peak at 1300 cm^{-1} is attributed to the F−C(sp3) stretching mode. In the case of the *x*-polarized IR signal (Figure 2), the 1300 cm^{-1} signal is seen only for the two-inner fluorine structure. Therefore, it can be used to identify this structure in combination with the 1150 cm^{-1} peak. Note, that the 1150 cm^{-1} peak is preferable for the current purpose, since it generates a stronger IR signal than the 1300 cm^{-1} vibration. Considering *y* polarized light (Figure 3a), we observe the F−C(sp3) stretching mode peak at 1300 cm^{-1} for all three structures. The location of the peak is slightly shifted; however, the shift is rather small, requiring a fine signal resolution and high quality samples.

Considering *z* polarized spectra, we observe a 1100 cm^{-1} peak that is characteristic of the all-outer fluorine structure. *Z*-polarized spectra involve motions out of the plane of graphene. By having all fluorine atoms on one side of the plane, one achieves the largest local out-of-plane distortion, creating a distinct signature of all-outer fluorinated graphene. At the same time, one cannot rely on this peak alone for identification of the all-outer structure, because fluorines penetrating through the graphene surface also create out-of-plane distortions, and therefore, generate smaller peaks in the same frequency regions.

Other peaks in the calculated IR spectra involve local F−C(sp3) bond vibrations and some C−C, C−F, and F−F

dx.doi.org/10.1021/jz201496q | *J. Phys. Chem. Lett.* 2012, 3, 246−250

collective motions. We avoid discussing these signals, since we cannot use them to distinguish between the different fluorinated structures.

Finally, we should mention that the 1150 cm^{-1} peak characteristic of two fluorine atoms attached to a C(sp3)−C(sp3) bond constitutes a robust IR feature that can be used to identify this pattern in larger carbon nanostructures of varying shapes and different degrees of distortion. At the same time, the 800 cm^{-1} peak associated with a single fluorine is less robust and may disappear in systems with large geometric and electronic distortions. This is because the frequency of the F−C(sp3) wagging motion may shift, or its intensity may decrease, due to sensitivity of this vibration to local environment. Additional analysis is required in order to explore the possibility to identify and distinguish the presence of isolated fluorine dopants in other types of carbon nanostructures.[34]

This study has demonstrated that IR spectroscopy can be used to distinguish between different fluorination patterns of graphene and related carbon nanostructures. Fluorination is commonly used as an intermediate chemical step during synthesis of more complex forms of graphene derivatives. It is also used to tune and control graphene's electronic, optical, and mechanical properties. The properties of the end product depend on the details and quality of fluorination, and the results reported here provide a straightforward route for detecting and characterizing different fluorination patterns.

Our calculations show that chains of graphene dopants can be detected by strong peaks around 1000 and 1500 cm^{-1} in the IR signal polarized along the chain direction. By penetrating into the inner surface of graphene, fluorine atoms create defects. Isolated fluorine defects can be identified by the 800 cm^{-1} peak in the IR spectrum. The peak originates from the local wagging motion of the F−C(sp3) bond. A pair of fluorine atoms generates a robust signal at 1150 cm^{-1}, produced by the local stretching motion of the bond formed by the C(sp3)−C(sp3) atoms connected to the fluorines. If the fluorine addition structures coexist, their ratio can be determined by the relative intensities of the spectral peaks associated with each structure.

The current analysis focused on the linear IR response function, which allowed us to successfully identify the inner- and outer-fluorine addition structures. Further information that is hard to deduce from the previous IR studies,[34,35] including coupling between the C−F bonds and structural defects, may be obtained by analysis of nonlinear response functions that are relevant for multidimensional vibrational spectroscopies.[36−40] The current study targeted single-layer graphene. Multilayer fluorinated carbon nanostructures have been predicted and investigated recently.[28,41−44] These materials show a number of interesting features that stem from interactions of fluorine atoms in different graphene layers. Our next study will investigate the IR signatures of these features in more detail.

AUTHOR INFORMATION

Corresponding Authors

*Tel: (+81)75-753-4019; e-mail: uetaakira@kuchem.kyoto-u.ac.jp; fax: (+81)75-753-4018 (A.U.). Tel: (+81)75-753-4017; e-mail: tanimura@kuchem.kyoto-u.ac.jp;fax: (+81)75-753-4018 (Y.T.). Tel: (+585)276-5664; e-mail: prezhdo@chem.rochester.edu; fax: (+585)276-0205 (O.V.P).

ACKNOWLEDGMENTS

The authors thank Daniel Packwood for useful comments. A.U. is supported by the research fellowship of the Global COE Program, International Center for Integrated Research, and Advanced Education in Material Science, Kyoto University. Y.T. is grateful for the financial support in the form of a Grant-in-Aid for Scientific Research B19350011 from the Japan Society for the Promotion of Science. OVP acknowledges the support of the U.S. is a Foreign Scholar of the Japan Society for the Promotion of Science and the CHE-1035196 grant of the National Science Foundation of the United States.

REFERENCES

(1) Kroto, H. W.; Heath, J. R.; O'Brien, S. C.; Curl, R. F.; Smalley, R. E. C-60: Buckminsterfullerene. *Nature* **1985**, *318*, 162−163.
(2) Kratschmer, W.; Lamb, L. D.; Fostiropoulos, K.; Huffman, D. R. Solid C_{60}: A New Form of Carbon. *Nature* **1990**, *347*, 354−358.
(3) Iijima, S. Helical Microtubules of Graphitic Carbon. *Nature* **1991**, *354*, 56−58.
(4) Prezhdo, O. V.; Kamat, P. V.; Schatz, G. C. *J. Phys. Chem. C* **2011**, *115*, 3195−3197.
(5) Rinzler, A. G.; Hafner, J. H.; Nikolaev, P.; Lou, L.; Kim, S. G.; Tomanek, D.; Nordlander, P.; Colbert, D. T.; Smalley, R. E. Unraveling Nanotubes: Field Emission from an Atomic Wire. *Science* **1995**, *269*, 1550−1553.
(6) Novoselov, K. S.; Geim, A. K.; Morozov, S. V.; Jiang, D.; Zhang, Y.; Dubonos, S. V.; Grigorieva, I. V.; Firsov, A. A. Electric Field Effect in Atomically Thin Carbon Films. *Science* **2004**, *306*, 666−669.
(7) Habenicht, B. F.; Craig, C. F.; Prezhdo, O. V. *Phys. Rev. Lett.* **2006**, *96*, 187401.
(8) Kilina, S.; Tretiak, S.; Doorn, S. K.; Luo, Z.; Papadimitrakopoulos, F.; Piryatinski, A.; Saxena, A.; Bishop, A. R. Cross-Polarized Excitons in Carbon Nanotubes. *Proc. Natl. Acad. Sci. U.S.A.* **2008**, *105*, 6769−6802.
(9) Kalugin, O. N.; Chaban, V. V.; Loskutov, V. V.; Prezhdo, O. V. Uniform Diffusion of Acetonitrile inside Carbon Nanotubes Favors Supercapacitor Performance. *Nano Lett.* **2008**, *8*, 2126−2130.
(10) Yarotski, D. A.; Kilina, S. V.; Talin, A. A.; Tretiak, S.; Prezhdo, O. V.; Balatsky, A. V.; Taylor, A. J. *Nano Lett.* **2009**, *9*, 12−17.
(11) Nelson, T.; Zhang, B.; Prezhdo, O. V. *Nano Lett.* **2010**, *10*, 3237−3242.
(12) Chaban, V. V.; Prezhdo, O. V. *ACS Nano* **2011**, *7*, 5647−5655.
(13) Tasis, D.; Tagmatarchis, N.; Bianco, A; Prato, M. Chemistry of Carbon Nanotubes. *Chem. Rev.* **2006**, *106*, 1105−1136.
(14) Kelly, K. F.; Chiang, I. W.; Mickelson, E. T.; Hauge, R. H.; Margrave, J. L.; Wang, X.; Scuseria, G. E.; Radloff, C.; Halas, N. J. Insight into the Mechanism of Sidewall Functionalization of Single-Walled Carbon Nanotubes: An STM Study. *Chem. Phys. Lett.* **1999**, *313*, 445−450.
(15) Jaffe, R. L. Quantum Chemistry Study of Fullerene and Carbon Nanotube Fluorination. *J. Phys. Chem. B* **2003**, *107*, 10378−10388.
(16) Lier, G. V.; Ewels., C. P.; Zuliani, F.; Vita, A. D.; Charlier, J. C. Theoretical Analysis of Fluorine Addition to Single-Walled Carbon Nanotubes: Functionalization Routes and Addition Patterns. *J. Phys. Chem. B* **2005**, *109*, 6153−6158.
(17) Mickelson, E. T.; Huffman, C. B.; Rinzler, A. G.; Smalley, R. E.; Hauge, R. H.; Margrave, J. L. Fluorination of Single-Wall Carbon Nanotubes. *Chem. Phys. Lett.* **1998**, *296*, 188−194.
(18) Kawasaki, S.; Komatsu, K.; Okino, F.; Touhara, H.; Kataura, H. Fluorination of Open- and Close-End Single-Walled Carbon Nanotubes. *Phys. Chem. Chem. Phys.* **2004**, *6*, 1769−1772.
(19) Claves, D.; Rossignol, J. Fluorine Addition to Single-Wall Carbon Nanotubes Revisited. *Chem. Phys. Lett.* **2009**, *468*, 231−233.
(20) Chamssedine, F.; Claves, D. Three Different Modes of Fluorine Chemisorption at the Surface of Single Wall Carbon Nanotubes. *Chem. Phys. Lett.* **2007**, *443*, 102−106.
(21) Peelaers, H.; Hernandez-Nieves, A. D.; Leenaerts, O.; Partoens, B.; Peeters, F. M. Vibrational Properties of Graphene Fluoride and Graphane. *Appl. Phys. Lett.* **2011**, *98*, 051914.
(22) Osuna, S.; Torrent-Sucarrat, M.; Sola, M.; Geerlings, P.; Ewels, C. P.; Lier, G. V. Reaction Mechanisms for Graphene and Carbon Nanotube Fluorination. *J. Phys, Chem. C* **2010**, *114*, 3340−3345.

(23) Wu, M.; Tse, J. S.; Jiang, J. Z. Unzipping of Graphene by Fluorination. *J. Phys. Chem. Lett.* **2010**, *1*, 1394−1397.
(24) Sahin, H.; Topsakal, M.; Ciraci, S. Structures of Fluorinated Graphene and Their Signatures. *Phys. Rev. B* **2011**, *83*, 115432.
(25) Bettinger, H. F.; Kudin, K. N.; Scuseria, G. E. Thermochemistry of Fluorinated Single Wall Carbon Nanotubes. *J. Am. Chem. Soc.* **2001**, *123*, 12849−12856.
(26) Lee, Y. S. Syntheses and Properties of Fluorinated Carbon Materials. *J. Fluorine Chem.* **2007**, *128*, 392−403.
(27) Claves, D.; Li, H.; Dubois, M.; Ksari, Y. An Unusual Weak Bonding Mode of Fluorine to Single-Walled Carbon Nanotubes. *Carbon* **2009**, *47*, 2557−2562.
(28) Robinson, J. T.; Burgess, J. S.; Junkermeier, C. E.; Badescu, S. C.; Reinecke, T. L.; Perkins, F. K.; Zalalutdniov, M. K.; Baldwin, J. W.; Culbertson, J. C.; Sheehan, P. E.; et al. Properties of Fluorinated Graphene Films. *Nano Lett.* **2010**, *10*, 3001−3005.
(29) Leenaerts, O.; Peelaers, H.; Hernandez-Nieves, A. D.; Partoens, B.; Peeters, F. M. First-Principles Investigation of Graphene Fluoride and Graphane. *Phys. Rev. B* **2010**, *82*, 195436.
(30) Prezhdo, O. V.; Kamat, P. V.; Schatz, G. C. Virtual Issue: Graphene and Functionalized Graphene. *J. Phys. Chem. C* **2011**, *115*, 3195−3197.
(31) Jeon, K. J.; Lee, Z.; Pollak, E.; Moreschini, L.; Bostwick, A.; Park, C. M.; Mendelsberg, R.; Radmilovic, V.; Kostecki, R.; Richardson, T. J.; et al. Fluorographene: A Wide Bandgap Semiconductor with Ultraviolet Luminescence. *ACS Nano* **2011**, *5*, 1042−1046.
(32) Brenner, D. W. Empirical Potential for Hydrocarbons for Use in Simulating the Chemical Vapor Deposition of Diamond Films. *Phys. Rev. B* **1990**, *42*, 9458−9471.
(33) Tanaka, J.; Abrams, C. F.; Graves, D. B. New C−F Interatomic Potential for Molecular Dynamics Simulation of Fluorocarbon Film Formation. *J. Vac. Sci. Technol. A* **2000**, *18*, 938−945.
(34) Ueta, A.; Tanimura, Y.; Prezhdo, O. V. Distinct Infrared Spectral Signatures of the 1,2- and 1,4-Fluorinated Single-Walled Carbon Nanotubes: A Molecular Dynamics Study. *J. Phys. Chem. Lett.* **2010**, *1*, 1307−1311.
(35) Luo, G.; Li, H.; Wang, L.; Lai, L.; Zhou, J.; Qin, R.; Lu, J.; Mei, W. N.; Gao, Z. Polarized Vibrational Infrared Absorption of Graphene Nanoribbons. *J. Phys. Chem. C* **2010**, *114*, 6959−6965.
(36) Nagata, Y.; Tanimura, Y.; Mukamel, S. Two-Dimensional Infrared Surface Spectroscopy for CO on Cu(100): Detection of Intermolecular Coupling of Adsorbates. *J. Chem. Phys.* **2007**, *126*, 204703.
(37) Hasegawa, T.; Tanimura, Y. Nonequilibrium Molecular Dynamics Simulations with a Backward−Forward Trajectories Sampling for Multidimensional Infrared Spectroscopy of Molecular Vibrational Modes. *J. Chem. Phys.* **2008**, *128*, 064511.
(38) Tanimura, Y.; Ishizaki, A. Modeling, Calculating, and Analyzing Multidimensional Vibrational Spectroscopies. *Acc. Chem. Res.* **2009**, *42*, 1270−1279.
(39) Nagata, Y.; Mukamel, S. Spectral Diffusion at the Water/Lipid Interface Revealed by Two-Dimensional Fourth-Order Optical Spectroscopy: A Classical Simulation Study. *J. Am. Chem. Soc.* **2011**, *133*, 3276−3279.
(40) Sakurai, A.; Tanimura, Y. Does $\hbar$ Play a Role in Multidimensional Spectroscopy? Reduced Hierarchy Equations of Motion Approach to Molecular Vibrations. *J. Phys. Chem. A* **2011**, *115*, 4009−4022.
(41) Dresselhaus, M. S.; Dresselhaus, G. Intercalation Componds of Graphite. *Adv. Phys.* **1981**, *30*, 139−326.
(42) Fan, X.; Liu, L.; Kuo, J. L.; Shen, Z. Functionalization Single- and Multi-Layer Graphene with Br and Br_2. *J. Phys. Chem. C* **2010**, *114*, 14939−14945.
(43) Ang, P. K.; Wang, S.; Bao, Q.; Thong, J. T. L.; Loh, K. P. High-Throughput Synthesis of Graphene by Intercalation − Exfoliation of Graphite Oxide and Study of Ionic Screening in Graphene Transistor. *ACS Nano* **2009**, *3*, 3587−3594.
(44) Withers, F.; Bointon, T. H.; Dubois, M.; Russo, S.; Craciun, M. F. Nanopatterning of Fluorinated Graphene by Electron Beam Irradiation. *Nano Lett.* **2011**, *11*, 3912−3916.